HOKKAIDO UNIVERSITY

Title	Algebraic Analysis Approach for Multibody Problems
Author(s)	Oikawa, Shun-ichi; Funasaka, Hideo
Citation	Plasma and Fusion Research, 3(S1073), S1073-1-S1073-5 https://doi.org/10.1585/pfr.3.S1073
Issue Date	2008
Doc URL	https://hdl.handle.net/2115/48801
Type	journal article
File Information	r2008_03-S1073.pdf

Hokkaido University Collection of Scholarly and Academic Papers : HUSCAP

Algebraic Analysis Approach for Multibody Problems

Shun-ichi OIKAWA and Hideo FUNASAKA

Graduate School of Engineering, Hokkaido University, N-13, W-8, Sapporo 060-8628, Japan

(Received 15 November 2007 / Accepted 7 March 2008)

Here we propose an algebraic analysis approach for multibody Coulomb interactions. The momentum transfer cross section calculated by the algebraic approximation is close to the exact one. The CPU time required for the algebraic approximation is only about 20 min using a personal computer, whereas the exact analysis requires 15 h to integrate the entire set of multibody equations of motion, in which all the field particles are at rest.

© 2008 The Japan Society of Plasma Science and Nuclear Fusion Research

Keywords: multibody problem, algebraic analysis, anomalous diffusion

DOI: 10.1585/pfr.3.S1073

1. Introduction

Since it is difficult to deal with multibody Coulomb and gravitational [1] collisions, the current classical theory considers them as a series of temporally-isolated binary Coulomb collisions within the Debye sphere. Let us first briefly review a binary collision between ions. In the center of mass coordinate (r, θ) space in the collision plane, the test particle with a reduced mass of μ moves along a hyperbola as

$$\boldsymbol{r}(\theta) = \frac{b \sin\theta_0}{\cos\theta - \cos\theta_0} \begin{bmatrix} \cos\theta \\ \sin\theta \end{bmatrix} \tag{1}$$

with a relative velocity of

$$\boldsymbol{g}(\theta) = \frac{g_0}{\sin\theta_0} \begin{bmatrix} \cos\theta_0 \sin\theta \\ 1 - \cos\theta_0 \cos\theta \end{bmatrix}, \tag{2}$$

from which the velocity change in the binary Coulomb interaction is given by $\Delta\boldsymbol{g} = 2g_0 \cos\theta_0 \boldsymbol{e}_x$. As shown in Fig. 1, its scattering angle $\chi \equiv \pi - 2\theta_0$ is given by $b = b_0 \tan\theta_0$, where b is the impact parameter, $b_0 \equiv e^2/4\pi\varepsilon_0\mu g_0^2$ corresponds to $\chi = \pi/2$ scattering, and g_0 is the initial relative speed at $r = \infty$ and $\theta = -\theta_0$.

The angular component of the equation motion gives the well-known invariant of

$$r^2 \frac{\mathrm{d}\theta}{\mathrm{d}t} = \text{const.} = b g_0, \tag{3}$$

and the radial component is given by

$$\frac{\mathrm{d}g_r}{\mathrm{d}t} = \frac{g_0^2 b_0}{r^2}\left(1 + \frac{b_0}{r}\tan^2\theta_0\right), \tag{4}$$

where $g_r \equiv \dot{r}$ denotes the radial velocity. The first term in the parentheses on the right hand side of Eq. (4) represents the Coulomb force $F_\mathrm{c} \propto r^{-2}$. For small angle scatterings such as $\chi \ll 1$, this force is much smaller than the second term F_a, which scales as $\propto r^{-3}$ and results from the conservation of angular momentum Eq. (3), since at the closest point $r = r_\mathrm{min}$ at $\theta = 0$ in Eq. (1), we have

$$\frac{b_0 \tan^2\theta_0}{r_\mathrm{min}} \simeq \frac{2}{\chi} \gg 1. \tag{5}$$

Thus the main force on the particle is not the Coulomb force F_c, but F_a due to the conservation of angular momentum.

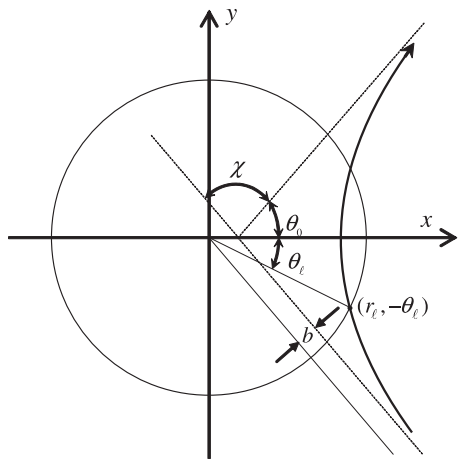

Fig. 1 Unperturbed trajectory $r = r(\theta)$ in an orbital plane. The scattering center is at the origin. An impact parameter is $b = b_0 \tan\theta_0$. Interaction region is inside the circle with a radius $r_\ell = \Delta\ell/2$.

2. Algebraic Approximation for Two-dimensional Multibody Interactions

Since the r-dependence on $F_\mathrm{a} \propto r^{-3}$ is steeper than that on $F_\mathrm{c} \propto r^{-2}$, the momentum change in $\mu\boldsymbol{g}$ is almost solely due to F_a near $r = r_\mathrm{min}$. As a consequence, the exact hyperbolic trajectory Eq. (1) for the particle can be approximated as a broken line with an impulse force of

$$\mu\Delta\boldsymbol{g} = 2\mu g_0 \cos\theta_0 \boldsymbol{e}_x \tag{6}$$

author's e-mail: oikawa@qe.eng.hokudai.ac.jp

© 2008 The Japan Society of Plasma Science and Nuclear Fusion Research

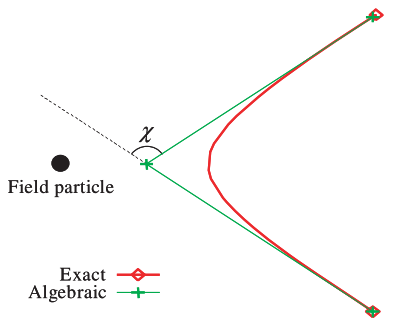

Fig. 2 Algebraic trajectory (broken line) and exact trajectory (curved line) which is a part of a hyperbola. A Field particle (black circle) is on the left.

near the closest point, as shown in Fig. 2.

With this in mind, we have approximated a multibody problem for a series of binary deflections near their closest point, as shown in Fig. 2, in which a test particle starts at the lower-right point, and its final point is at the upper-right point due to the interaction with a field particle at rest.

The *exact* calculation hereafter refers to that obtained by solving the following equation of motion for the test particle with a charge e, mass m, and velocity $\boldsymbol{v}$ at a position $\boldsymbol{r}$.

$$\frac{\mathrm{d}\boldsymbol{v}}{\mathrm{d}t} = \frac{e^2}{4\pi\varepsilon_0 m} \sum_{i=-N}^{N} \sum_{j=-N}^{N} \frac{\boldsymbol{r} - \boldsymbol{r}_{ij}}{\left|\boldsymbol{r} - \boldsymbol{r}_{ij}\right|^3}, \tag{7}$$

where $\boldsymbol{r}_{ij}$ are the field particles' positions determined by the 5-th order Runge-Kutta-Fehlberg method, which is also known as the RKF56.

For simplicity, let us assume, that all the filed particles are at rest, i.e., $\boldsymbol{v}_{ij} = \boldsymbol{0}$, in the x–y plane. Let us also assume that their spatial distribution $\boldsymbol{r}_{ij}$ is almost uniform with a spacing of the average interparticle separation $\Delta\ell \equiv n^{-1/3}$, as

$$\boldsymbol{r}_{ij} = \left(i\,\Delta\ell + \delta x_{ij}\right)\boldsymbol{e}_x + \left(j\,\Delta\ell + \delta y_{ij}\right)\boldsymbol{e}_y,$$

for $-N \le i,\ j \le N$, as shown in Fig. 3, where n stands for the number density, and deviations $\delta\boldsymbol{r}_{ij} = \left(\delta x_{ij}, \delta y_{ij}\right)$ from grid points $(i\Delta\ell,\ j\Delta\ell)$ satisfy

$$\left.\begin{aligned} &\delta x_{ij} = \delta y_{ij} = 0 \quad (\text{for } i = j = 0) \\ &\sum_{i,j}^{N\to\infty} \delta x_{ij} = \sum_{i,j}^{N\to\infty} \delta y_{ij} = 0 \quad (\text{else}) \end{aligned}\right\}, \tag{8}$$

and

$$\frac{1}{N_\mathrm{p}} \sum_{i,j}^{N\to\infty} \delta x_{ij}^2 = \frac{1}{N_\mathrm{p}} \sum_{i,j}^{N\to\infty} \delta y_{ij}^2 \sim \Delta\ell^2. \tag{9}$$

The first assumption in Eq. (8) states that the field particle with $i = j = 0$ is always at the origin in this study, i.e. $\boldsymbol{r}_{00} = 0$. The impact parameter b is for the field particle at the origin, i.e., $b = b_{00}$, as shown in Fig. 3. It should be noted that the number N is not the number of field particles, N_p, which is given by $N_p = (2N+1)^2$.

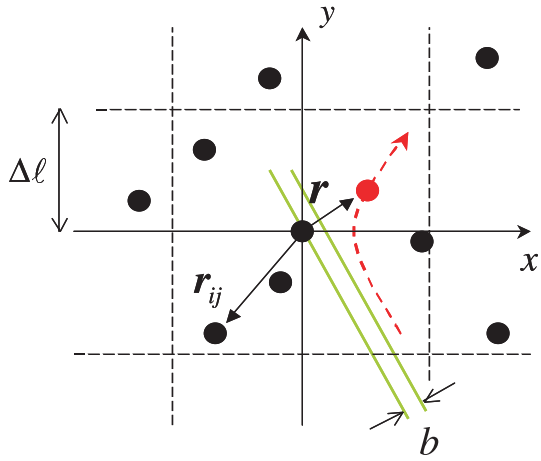

Fig. 3 Two-dimensional multibody Coulomb interaction. A gray circle (or red in color) is a test particle at $\boldsymbol{r}$ with an impact parameter b, and almost-uniformly-distributed black circles are field particles.

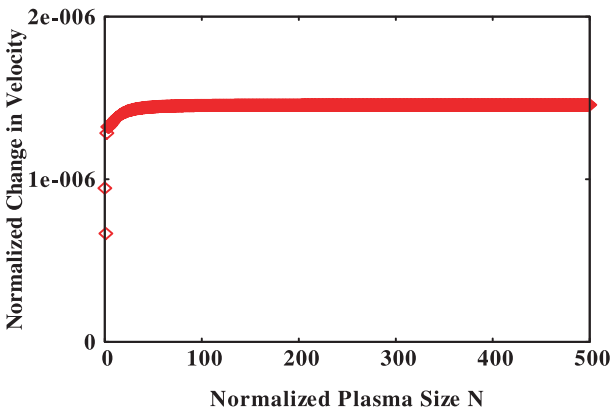

Fig. 4 An example of the *exact* velocity changes vs nondimensional plasma size N. The impact parameter $b = \Delta\ell/5$ and the field particle positions are fixed.

In typical fusion plasmas with a temperature of $T = 10$ keV and a number density of $n = 10^{20}$ m^{-3}, the Debye length is $\lambda_\mathrm{D} \sim 500\ \Delta\ell$, thus $N \sim 500$ corresponds to λ_D. Figure 4 shows N-dependence of the *exact* velocity changes Δv_x for a fixed impact parameter $b = \Delta\ell/5$ and for fixed positions of N_p field particles [2]. After the equation of motion for a test particle is solved in the presence of N_p field particles for an N with $0 \le N < N^{\max} \equiv 500$, we increase N as $N = N + 1$ without changing the positions of N_p field particles, which are already considered in the previous N-th stage of the analysis. In Fig. 4, the velocity change is seen to converge around $N = 10$, which we adopt in the following calculations.

2.1 Coordinate transformation

In order to apply the above approximated binary interaction shown in Fig. 2 to a multibody case shown in Fig. 3, we first seek for a field particle that provides the test particle with an impulse force *at the earliest time*. For this

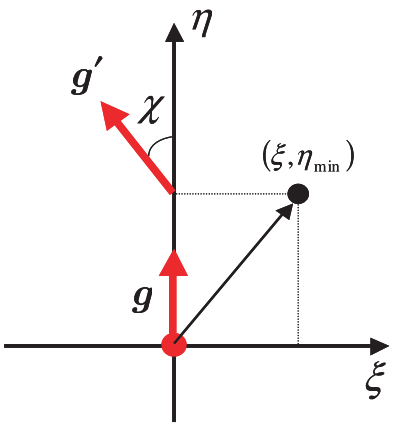

Fig. 5 Coordinate transformation.

purpose, it is convenient to transform the coordinate system from (x, y) to (ξ, η), such that the initial position of the test particle is at the origin $(\xi, \eta) = (0, 0)$, and the relative velocity $\boldsymbol{g} \equiv \boldsymbol{v} - \boldsymbol{v}_{ij}$ is $(g_\xi, g_\eta) = (0, g)$. Then a field particle at $\boldsymbol{r}_{ij}$ has an η-coordinate of

$$\eta_{ij} = \left(\boldsymbol{r}_{ij} - \boldsymbol{r}\right) \cdot \boldsymbol{g}/g. \tag{10}$$

The test particle moves along the η-axis with a constant velocity g, and is to interact at $\left(0, \eta_{ij}\right)$ with this field particle in a time interval of $\Delta t_{ij} \equiv \eta_{ij}/g$ s. Accordingly, the field particle that provided the test particle with an impulse force at the earliest time has the smallest positive η_{ij}, i.e.,

$$\eta_{\min} \equiv \min(\max(0, \eta_{ij})), \text{ for } -N \le i, j \le N. \tag{11}$$

We have ignored the effect of field particles with $\eta_{ij} < 0$, since the interaction is completed at $\eta = 0$ in our approximation. In other words, such field particles have already interacted with the test particle in the past.

When the test particle moves to $(0, \eta_{\min})$ position, it changes the relative velocity by $\Delta \boldsymbol{g}_{ij}$ as

$$\Delta \boldsymbol{g}_{ij} = -2g \sin \frac{\chi_{ij}}{2} \boldsymbol{e}_\xi, \tag{12}$$

$$\chi_{ij} \simeq 2 \arctan \frac{b_0}{\xi_{ij}}, \tag{13}$$

where the pair of i and j satisfies Eq. (11), and we have approximated that the impact parameter is given by $b = \xi_{ij}$ in Eq. (6), as shown in Fig. 5. Thus, in the (ξ, η) coordinate system, the field particle positions, ξ_{ij} and η_{ij}, correspond to the velocity change $\Delta \boldsymbol{g}_{ij}$ and the time of the interaction Δt_{ij}, respectively. This procedure is repeated until the test particle leaves the prescribed interaction region, i.e., $r < \Delta\ell/2$, as depicted in Fig. 1.

3. Calculation

3.1 Comparison between the exact and algebraic trajectories

Figure 6 compares the algebraic trajectory and the exact hyperbola in the case of the pure binary Coulomb interaction, i.e., $N = 0$ in Eq. (7), with an impact parameter $b = \Delta\ell/5$. The only field particle is at the origin in this case. The test particle starts at the lower right point, passes through the closest point, and ends at the upper right point in the figure.

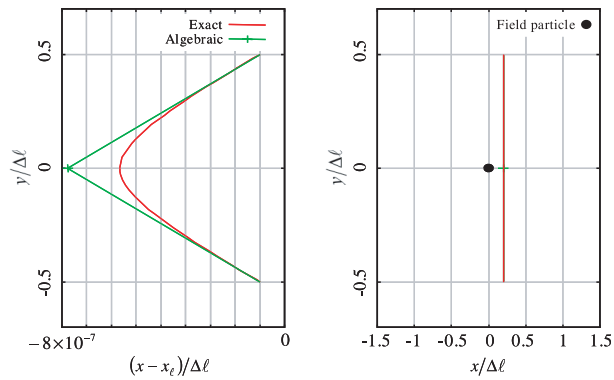

Fig. 6 Comparison of algebraic trajectory and exact trajectory in the case of binary Coulomb collision ($N = 0$) with an impact parameter $b = \Delta\ell/5$. In the figure on the right, the exact- and algebraic trajectories are depicted with the only field particle at the origin, in which the field particle location is also shown with a black circle. On the left is the enlarged view.

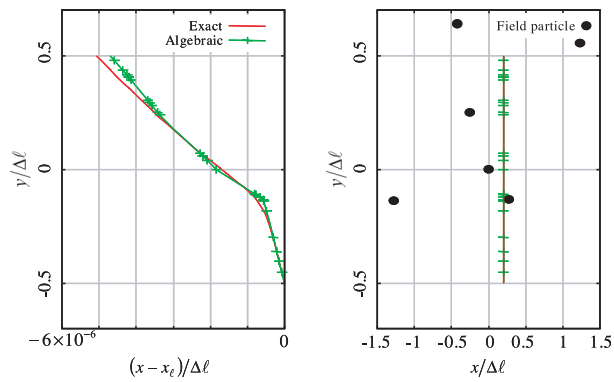

Fig. 7 Comparison of algebraic trajectory and exact trajectory in the case of multibody ($N = 10$) Coulomb collisions with an impact parameter $b = \Delta\ell/5$. Note that not all the field particles are shown. This is an example of small angle scatterings.

Figures 7, 8, and 9 are three examples out of 10^5 Monte Carlo calculations for an impact parameter $b = \Delta\ell/5$, and they compare the algebraic and exact trajectories in the case of the multiple Coulomb interactions, i.e., $N = 10$ in Eq. (7). In these cases, there are nearly uniformly distributed 21×21 field particles at rest, and symbols in the figures for the algebraic trajectories indicate the positions at which the test particle is provided with the impulse force by one of the N_p field particles. Individual approximations are good in most cases, as shown in Figs. 7 and 8. The former is an example of small angle scattering, and the latter depicts the large angle scattering case. On the other hand, Fig. 9 is one of few examples in which the

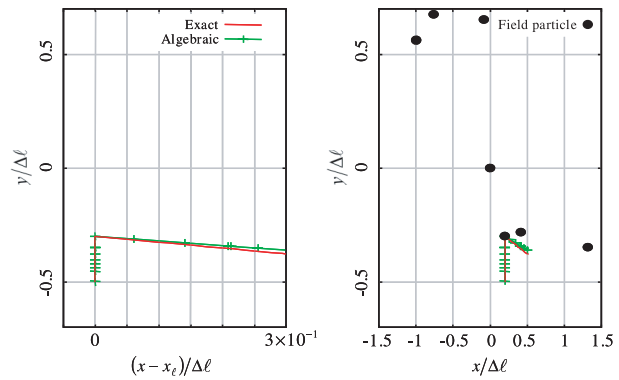

Fig. 8 Comparison of algebraic trajectory and exact trajectory in the case of multibody ($N = 10$) Coulomb collisions with an impact parameter $b = \Delta\ell/5$. This is an example of large angle scatterings.

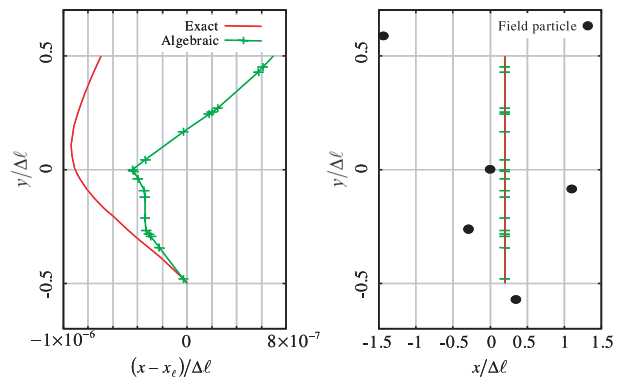

Fig. 9 Comparison of algebraic trajectory and exact trajectory in the case of multibody ($N = 10$) Coulomb collisions with an impact parameter $b = \Delta\ell/5$. The discrepancy is as small as 10^{-13} meter in typical fusion plasmas.

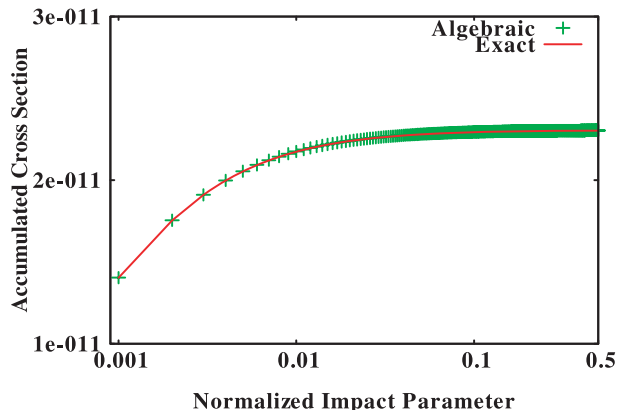

Fig. 10 Accumulated binary ($N = 0$) Coulomb scattering cross section $\sigma_{\rm acc}^{\rm bin}(b)/\Delta\ell^2$ vs normalized impact parameter $\bar{b} = b/\Delta\ell$.

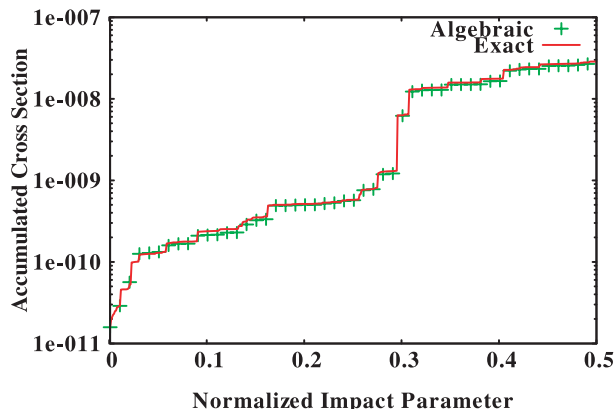

Fig. 11 Accumulated multiboby ($N = 10$) Coulomb scattering cross section $\sigma_{\rm acc}^{\rm multi}(b)/\Delta\ell^2$ vs normalized impact parameter $\bar{b} = b/\Delta\ell$.

approximation seems bad. The algebraic trajectory in Fig. 9 deviates from the exact one, however, the deviation is as small as $\Delta\ell\times10^{-6} \sim 10^{-13}$ meter in typical fusion plasmas, which is of the same order of the de Broglie wavelength.

3.2 Momentum transfer cross section

Finally, we conducted the above calculation for different impact parameters $0 < b < \Delta\ell/2$. Figure 10 shows the accumulated variance of velocity change $\left\langle(\Delta\boldsymbol{g})^2\right\rangle$, which is in proportion to the momentum transfer cross section, $\sigma_{\rm m}^{\rm bin}$, as

$$\sigma_{\rm m}^{\rm bin} = \int_0^{b_{\rm max}} \left(\frac{\Delta\boldsymbol{g}}{g}\right)^2 \pi b{\rm d}b = 4\pi b_0^2 \ln\frac{b_{\rm max}}{b_0}. \qquad (14)$$

Depicted in Fig. 10 is the *accumulated* scattering cross section $\sigma_{\rm acc}(b)$ as a function of the impact parameter b defined by

$$\sigma_{\rm acc}(b) = \int_0^{b} \left(\frac{\Delta\boldsymbol{g}}{g}\right)^2 \pi b{\rm d}b. \qquad (15)$$

The error in the accumulated cross section $\sigma_{\rm acc}^{\rm bin}(b)$ due to the algebraic approximation is quite small for the binary ($N = 0$) case, as shown in Fig. 10, where there is only one field particle. It should be noted that in the binary interactions, the cross section $\sigma_{\rm acc}^{\rm multi}(b)$ is converged at $b \ll \Delta\ell$, which is far less than the Debye length $\lambda_{\rm D} \sim 500\Delta\ell$ in fusion plasmas.

In the case of the multibody ($N = 10$) interaction, where there are 21×21 field particles, the error in $\sigma_{\rm acc}^{\rm multi}(b)$ is quite small, as shown in Fig. 11.

4. Discussion

The two-dimensional multibody scattering cross section $\sigma_{\rm acc}^{\rm multi} \simeq 2.8\times10^{-8}\Delta\ell^2$ with the maximum impact parameter $b_{\rm max} = \Delta\ell/2$ is more than 10^3 times the binary cross section $\sigma_{\rm acc}^{\rm bin} \simeq 2.3\times10^{-11}\Delta\ell^2$. However, this is not the anomalous diffusion. The binary interaction occurs in an orbital plane, whereas multibody interactions are inherently three-dimensional. Even if a field particle locates so close to the test particle in the (x, y) plane that the interaction results in a large angle scattering in the 2-d calculation with, say, $z \equiv 0$, the same field particle locates not neces-

sarily close to the test particle with $z \neq 0$ in 3-d.

The CPU time required for the algebraic approximation is only about 20 min using a personal computer, whereas the exact analysis requires 15 h to integrate the entire set of multibody equations of motion.

Strictly speaking, the analysis here is not for multibody problems, but solves the test particle motion in the presence of the multiple field particles at rest. The extension to the full multibody problem is straightforward. We will soon apply this method to three dimensional full multibody interactions.

[1] J. Makino and M. Taiji, APJ **480**, 432-446 (1997).
[2] H. Funasaka, Master thesis, Division of Quantum Science and Engineering, Hokkaido University (2007).